Controlling Electron Transport Rate and Recombination Process of Indigo Carmine Dye-Sensitized Solar Cells by Design of Composite TiO_2 Nanowires/Nanoparticles Photoanodes

N. G. Joby[1], P. Venkatachalam[2]* and N. Krishnakumar[1]

Abstract

Nanostructured films of metal-oxide semiconductors are the focus of intensive research nowadays due to their applications in the current quest for new sources of clean energy. Metal-oxides like TiO_2 can be used to make efficient photoanodes for photoelectrochemical solar cells. Dye-sensitized solar cells (DSSCs) are an attractive solar cell option because of their relatively low manufacturing costs and simple process technology. In the present investigation, DSSC based on TiO_2 nanowires/nanoparticles composite photoanodes were prepared. TiO_2 nanowires (TNWs) are prepared via hydrothermal treatment and the photoanodes are made-up of by mixing various mass ratios of TiO_2 nanowires with TiO_2 nanoparticles (TNPs). DSSCs photoanode were prepared using TNWs concentrations of 0%, 10%, 50%, 90% & 100% with TNPs and are named as DSSC-2, DSSC-3, DSSC-4, DSSC-5 & DSSC-6 respectively. In addition, a photoanode is prepared using bulk particle of TiO_2 and named as DSSC-1. In this work, Indigo carmine dye is used as a photo sensitizer, PMII (1-propyl-3-methylimmidazolium iodide) ionic liquid as electrolyte and Copper sulfide is used in counter electrode. The morphology of TiO_2 nanowires with nanoparticles would be a promising nanostructure in fabricating DSSCs for its advantages in charge separation, electronic transport and light harvesting. The results of the present investigation revealed that the composite photoanode containing optimized TiO_2 nanowires with nanoparticles can increase electron transfer efficiency. Among all DSSCs, DSSC-3 (TiO_2 nanowires content is 10 wt%) have illustrated the relative high conversion efficiency of 3.04% because of the longer electron life time and rapid electron transfer in the photoanode and electrolyte regions of this cell. This work has established that composite TNWs/TNPs photoanode structure can suppress the electrons recombination process and increase the conversion efficiency effectively.

Keywords: DSSCs, TiO_2 NWs, NPs, sol-gel process, hydrothermal process, X-ray diffraction, electron microscopy, EIS

1. INTRODUCTION

Increasing demand for energy is forcing us to research into new resources, among which solar energy is ideal to meet the target because of its abundant, clean and inexhaustible characteristics. New concepts in photovoltaics, photocatalysis and energy storage, attracting extraordinary interest from researchers and technologists nowadays, are based on the unique properties of nanostructured materials. The decisive advantage of nanostructured morphology is that it provides a high surface to volume ratio while maintaining some of the basic properties of the bulk material and adding new exciting ones [1]. Dye-sensitized solar cells (DSSCs) have been recognized as an attractive alternative to conventional solid-state homo and hetero junction solar cells because of their reasonable solar-to electricity conversion efficiency and simple fabrication on rigid and flexible substrates [2], [3], [4], [5], [6], [7]. DSSC is comprised of self-organized metal oxide nano structured conducting substrate offer (a) large surface areas for dye sensitization, which results in enhanced light harvesting; (b) easy transfer of electrons injected from the photo-excited dye; (c) vectorial (directed) charge transport to the electrical contact; and (d) a readily accessible space for intercalation of the redox electrolyte. Morphology of photoanode in the nanoscale is a key issue of DSSCs [2], [8], [9], where the high surface area ensures a large concentration of the light absorber material leading to good light harvesting and an intimate contact with the electron and hole transporter material [10]. In recent years, one-dimensional (1D) array materials, such as nanotubes, nanorods, and nanowires, have been successively synthesized and applied to improve the electron transportation ability in DSSCs [11], [12], [13], [14]. These 1D array materials can offer direct pathways for electron transport, thus the electron transport in them is several orders of magnitude faster than that in the case of nanoparticle films, suggesting lower opportunities of photogenerated electrons recombination [15], [16]. Therefore, it is highly desirable to synthesize 1D structure with high surface area and good light-scattering ability simultaneously.

[1]*Department of Physics, Annamalai University, Annamalainagar, TamilNadu, INDIA*
[2]**Department of Physics (DDE), Annamalai University, Annamalainagar, TamilNadu, INDIA*
e-mail: pvchalamphyamu@yahoo.co.in
Ph: +91 9443279865

Metal oxide films have been demonstrated to be promising candidate as photoanodes due to their appropriate energy band position and both thermal and chemical stability in solution. Nano structure TiO_2 has got wide band gap and large surface area, so that it can absorb maximum amount of photons from the sunlight. TiO_2, particularly in the anatase form, is a photocatalyst under sunlight. Traditional DSSCs use high-surface-area titania nanocrystalline thin films as the photosensitized anode material and a power conversion efficiency of 11.18% has been achieved [17]. However, a further increase in the conversion efficiency is impeded by slow electron percolation and recombination loss resulting from electron trap states that reside on the surface of the disordered nanoparticle network [15], [18], [19], [20]. The rapid electron transport in the TiO_2 film is important to ensure their efficient collection by the conducting substrate when in competition with the recombination processes and the electrons transport through a slow trap-limited diffusion process [21]. TiO_2 nanowire (TNWs) has got large surface area, environmentally benign component, improved light scattering and electron transport, all of which contribute toward improving key characteristics of low cost and high efficiency.

In DSSC, the sensitizer is one of the key components for high power-conversion efficiency. In recent years, much interest in metal-free organic dyes as an alternative to noble metal complexes has increased due to many advantages, such as diversity of molecular structures, high molar extinction coefficient, simple synthesis as well as low cost and environmental issues. The requirements of sensitizer should be good photo response in the visible region, high long-term stability under sun soaking, and appropriate lowest unoccupied molecular orbital (LUMO) levels matching the conduction band of TiO_2. In this work, Indigo carmine dye is used as a photo sensitizer for DSSC fabrication. The use of ionic liquid electrolyte is advantageous due to the high degree of wetting obtained on the fused nanoporous metal oxide electrode as well as its high ionic conductivity. However, encapsulation of volatile organic electrolytes with high vapor pressure is a major challenge in practical applications of the DSSC. Room temperature ionic liquids (ILs) are an attractive class of molecules for their utilization as electrolytes in DSSCs due their low volatility and high ionic conductivities. In the counter electrode, cobalt sulfide is used which is far less expensive, more efficient, more stable and easier to produce in the laboratory.

In the present investigation, TNPs were synthesized by sol-gel method and TNWs were prepared through an alkali hydrothermal transformation. The photoanodes were prepared using composites of anatase TiO_2 nanowires with TiO_2 nanoparticles in the fabrication of DSSCs. Working photo electrodes were arranged using TNWs concentrations of 0%, 10%, 50%, 90%, and 100% with TNPs and are represented as DSSC-2, DSSC-3, DSSC-4, DSSC-5 & DSSC-6 respectively. In addition, a photoanode is prepared using bulk particle of TiO_2 and is named as DSSC-1.This TNWs structure is expected to facilitate the electron transportation within the photo anode layer and enhance efficiency of DSSCs.

2. EXPERIMENTAL

All chemicals used in this study were of high purity which were purchased from Sigma-Aldrich, India and were used without further purification unless otherwise stated. TiO_2 NPs and NWs composite paste were coated uniformly onto ITO glass by the doctor blade technique of thickness ~ 12μm.

2.1 Preparation of TiO_2 Nanoparticles and Nanowires

TiO_2 NPs was synthesized using titanium (IV) isopropoxide [TTIP], nitric acid, ethyl alcohol, and distilled water. The TTIP was mixed with ethanol and distilled water was added drop by drop under vigorous stirring for 1 h. This solution was then peptized using nitric acid and heated under reflux at 80° C for 8 h. After this period, a TiO_2 sol was prepared. The prepared sol was dried to yield a TiO_2 powder. The TiO_2 particles were calcined at 450°C for 1 h in a furnace to obtain the desired TiO_2 stoichiometry and crystallinity [22]. TNWs were prepared through hydrothermal process. 2g of TiO_2 NPs particles as prepared by the sol-gel method were mixed with 100 ml of a 10-M NaOH aqueous solution, followed by hydrothermal treatment at 150°C in a Teflon-lined autoclave for 12 h. After the hydrothermal reaction, the treated sample was washed thoroughly with distilled water and 0.1 M HCl and subsequently filtered and dried at 80°C for 1 day. To achieve the desired TNW size and crystallinity, the sample was calcined at 600°C for 1 h [23].

2.2 Preparation of Indigo carmine dye

Natural indigo fresh plant root was washed with water and made into powder. The powder is mixed in boiling water and maintains 2–3 h, and the solids were filtrated out. Now the solution is opaque and blue color. Adding 1g of sodium hydroxide and 1 g of thiourea dioxide in the stock solution and kept at temperature of 80° C for 1 h [24]. The resulting stock solution is treated with sulfuric acid, which converts indigo into blue-green derivative called indigo carmine (sulfonated indigo).

2.3 Fabrication of DSSC Cells

The TiO_2 pastes with various ratios of NPs/NWs were prepared by ultrasonically mixing for 2 h. The as-prepared pastes were deposited by doctor-blade technique on indium-doped tin oxide conducting glass (ITO, 8-10Ω/square) by preparing an active area of 4 cm^2. Five pastes of TiO_2 NWs concentrations of 0%, 10%, 50%, 90%, and 100%, with NPs were used to prepare photoanode, which were respectively labeled as DSSC-2, DSSC-3, DSSC-4, DSSC-5 and DSSC-6. One more DSSC was fabricated using bulk particle of TiO_2 represented as DSSC-1. Thickness of the films was controlled by adjusting the thickness of adhesive tapes (here the thickness of the photoanode film after calcinations is about ~12 μm). The film is then heated to 500°C at a rate of 15°C /min and kept at 500°C for 30 min. After cooling to 80°C, the TiO_2 working electrode is immersed overnight in a solution of Indigo carmine dye. One drop of iodine-containing electrolyte was deposited onto the surface of the electrode and penetrated inside the TiO_2 film via capillary action. The electrolyte was composed of 0.6 M 1-methyl-3-propylimidazolium iodide (PMII), 0.1 M LiI, 0.05 M I_2, 0.5 M tert-butylpyridine in acetonitrile. A copper sulfide counter electrode was then clipped on top of the TiO_2 photoanode to form a photovoltaic device.

The photovoltaic properties of the DSSCs were characterized by recording the photocurrent and voltage (I-V) curves under illumination of A.M. 1.5 G (100 mW/cm^2). TiO_2 NPs and NWs were characterized by X-ray diffraction (XRD) using X-ray diffractometer (X'Pert PRO-PANalytical, Philips). Transmission electron microscopy (TEM) characterization was taken by (JEOL JSM-100CX) electron microscope. Specific area of the TiO_2 was determined by Brunauer-Emmett-Teller (BET) method using Accelerated Surface Area and Porosimetry Analyzer (Micromeritics ASAP-2020, USA). Photo electrochemical characteristics and the ac impedance measurements of the DSSCs were recorded with a LCZ Meter- Keithley, USA. The applied bias voltage and ac amplitude were set at open-circuit voltage of the DSSCs and 10mV between the ITO/CS counter electrode and the ITO/TiO_2/dye working electrode, respectively, and the frequency range explored was 1mHz to 10^5 Hz. The impedance spectra were analyzed by an equivalent circuit model for interpreting the characteristics of the DSSCs.

3. CHARACTERIZATION AND MEASUREMENTS

3.1 XRD, TEM and SEM analysis

The structures and morphologies of the TiO_2 NPs and NWs were characterized by XRD and TEM. Fig. 3.1 (a) shows the XRD patterns of TNPs and Fig. 3.1 (b) shows the XRD patterns of TNWs after annealing at 600 °C respectively. The peaks of (101), (004), (200), (105) and (211) are typical peaks of anatase TiO_2 [JCPDS: PDF#21-1272]. From this Fig.3.1, it could be noticed that the TiO_2 NPs and NWs exhibit an anatase structure with no impurity phase. The enhanced peaks indicate that the TNWs are well crystallized. Fig. 3.2 (a) and Fig. 3.2 (b) shows the TEM image of TiO_2 NPs and NWs respectively. The average diameter of the TNPs is 10-20nm. From the Fig. 3.2 (b), it can be found that the TiO_2 nanowire has smooth surface after calcination, with nearly uniform in diameter along its length, which suggests that the nanowire grows through epitaxial addition of growth units to the tips [25].

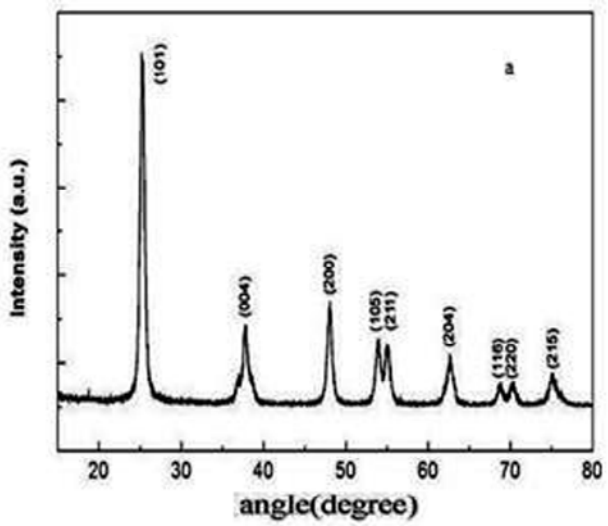

Fig 3.1 (a) XRD pattern of TiO_2 NPs

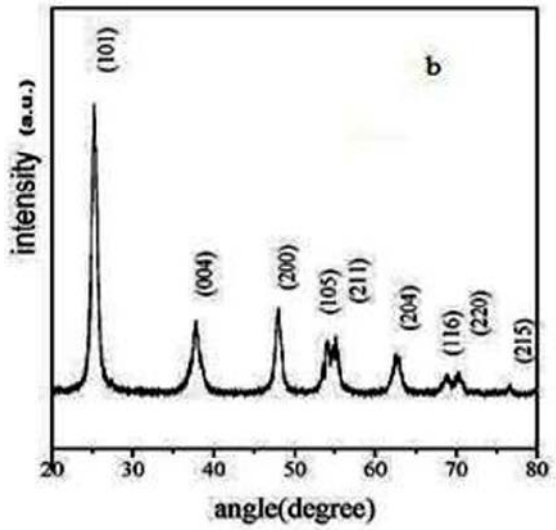

Fig 3.1 (b) XRD pattern of TiO_2 NWs

TEM image indicates that TiO_2 nanowire having diameter ranging from tens to hundreds nanometers. The Brunauer-Emmett-Teller (BET) surface area of the TiO_2 nanowires is 80 m^2 g^{-1}. This value is much higher than that of TiO_2 nanoparticles (ca.20m^2 g^{-1}). Most of the NWs have the length of a few microns and they are very uniform, quite clean, and smooth-surfaced. It can be seen the starting material exhibits nanoparticles type and the mean diameters are about 10-20 nm after hydrothermal synthesis, the particles were completely converted to TiO_2 nanowires. The texture of the NWs is uniform and reasonably dense though there are ample voids between the wires.

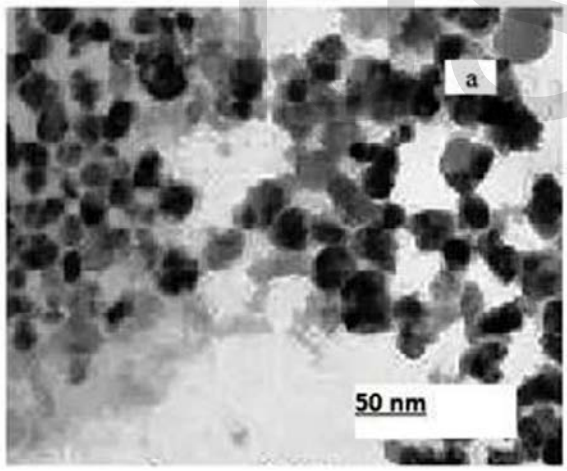

Fig 3.2 (a) TEM photograph of TiO_2 NPs

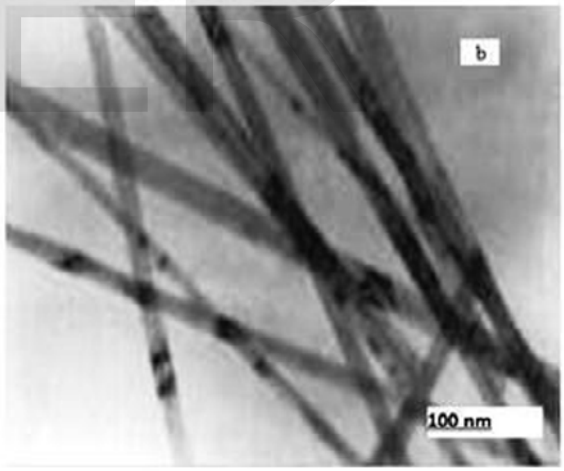

Fig 3.2 (b) TEM photograph of TiO_2 NWs

3.2 Photovoltaic Performances

The photocurrent-voltage (I-V) characteristics of the DSSCs with various concentrations of TNWs with the TNPs in the photoanodes are shown in Fig. 3.4. The detailed photovoltaic parameters open-circuit voltage (V_{OC}), short-circuit photocurrent density (I_{SC}), fill factor (FF) and energy conversion efficiency (η) of the DSSCs are listed in Table 3.1. The overall energy conversion efficiency of DSSCs is varied with the concentration of TiO_2 NWs with TNPs. The DSSC-1 is made using only bulk particle of TiO_2 showed lowest efficiency. Photovoltaic parameters for the TNPs DSSC-2 are V_{OC} = 840 mV, I_{SC} = 11 mA, FF = 72.08%, and η = 1.67%. By incorporation of NWs (10%) into the TiO_2 films, the V_{OC} value changes dramatically from 840 to 880 mV as the concentration of NWs increases. Also, the I_{SC} and FF value of the cells also increased when the NWs were

employed. As a result of the good photovoltaic parameters for the cell consisting of TNWs/TNPs composites, the highest η of 3.04% is obtained for DSSC -3 at an optimized condition where the TNWs percentage is 10%. Compared with the DSSC-2, based on pure TNPs, an increase of ~ 82% is achieved. Furthermore, V_{OC} is improved from 840mV to 880mV with enhancing the TNWs weight content in the TNPs based electrode from 0 to 10%. Generally, V_{OC} of a solar cell is determined by the difference between the Fermi level for electrons in the TiO_2 electrode and the redox potential of I_3^-/I^-. As can be seen in Table 3.1, I_{SC} shows an increasing behaviour first from 11 mA to 17.1 mA when the nanowire content is 10 wt %. Once the nanowire content exceeds 10 wt %, I_{SC} starts to drop dramatically from 17.1 mA to 10.3 mA. The dependence of η on the nanowire content is consistent with that of I_{SC}, which achieves the maximum energy conversion efficiency 3.04% at the 10 wt % nanowire and then decreases when the nanowire content is greater than 10 wt %. In the case of nanostructure working electrode, the DSSC with TNW electrode (DSSC-6) exhibits the lowest value of I_{SC} and η, which implies that pure nanowire structure, may block the transport of electrons in the photoanode. DSSCs fabricated with electrodes containing the composite TNWs with TNPs display higher V_{OC}, I_{SC}, FF and η as compared to the solar cell based on a pure TNPs electrode. Due to the one-dimensional structure of the TNWs, the charge recombination could decrease and charge transfer rate increases because of its straight charge transfer path divided by the nanowires, which result in an increase of electron density in TiO_2 electrode. It is reasonable to think the relatively larger size of the nanowires than NPs could enlarge the pore size of the film to improve the diffusion of liquid electrolyte, which is beneficial for electron transfer in I_3^-/I^- electrolyte [26].

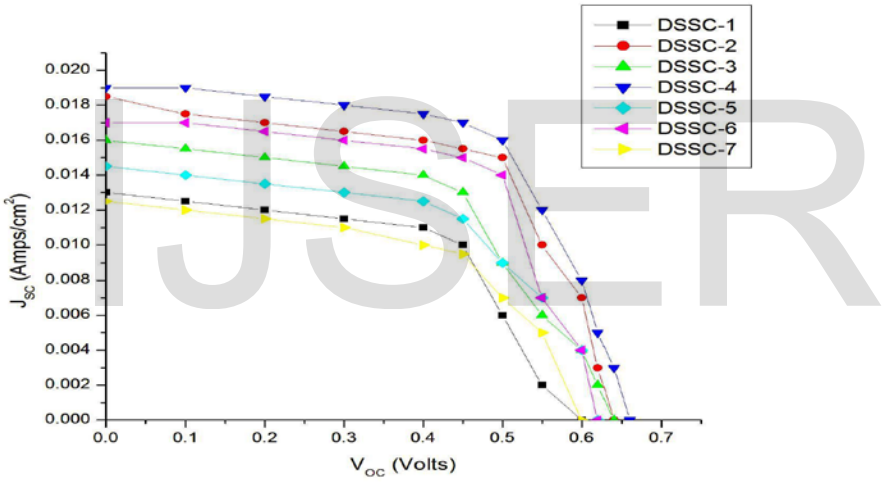

Fig 3.4 I-V characteristics of DSSC

The low electron recombination and fast electrolyte diffusion are beneficial for lowering the concentration of I_3^-/I^-, and the V_{OC} depends logarithmically on the inverse concentration of I_3^- [27]. Consequently, the V_{OC} increases with enhancing the nanowires weight content in the NP based electrodes at 10% wt, afterwards V_{OC} is decreased slowly with increasing nanowire concentration. DSSC made of pure TNPs photoanode, the injected electrons diffuse through the sintered nanoparticles film, through a series of inter particle hopping steps until they reach the collector electrode. While electrons within individual particles are highly mobile, the numerous nanoparticles boundaries and dead-ends in the disordered network limit microscopic electron transport [28]. This restricted transfer of electrons in the case of the film with TNPs is probably the reason for the relatively low I_{SC} and FF of its cell. The electron transferring in pure TNPs film, composed of random particles is expected to be limited by electron traps, and this can increase the recombination between the conduction band electrons in the TNPs and I_3^- in the electrolyte, and thereby can decrease the pertinent V_{OC}. With relatively low I_{SC}, V_{OC}, η and FF, the cell with TNPs shows a small light-harvesting efficiency of 1.67%. Obviously, the DSSC with the composite film of TNWs/TNPs shows the better performance in this study. For the photoanode with this composite structure, the nanowires in the film could provide direct pathways for electrons transfer, as the nanowires have a regular structure perpendicular to the electrode; it can be visualized that photoelectrons can travel along the direction parallel to the nanowires, i.e.,

precisely in the direction of the collecting electrode. In addition, the light scattering effects of the TNWs could favour enhanced light-harvesting efficiency, and thereby enhanced I_{SC} for the cell with the composite film. The coverage of the TNWs with the TNPs endows adequate surface area for the composite film and thus favours high dye-adsorption for the photoanode and high I_{SC} for the cell. Faster electron transfer in the composite film of TNWs/TNPs is considered as the reason for the higher FF of the cell with the composite film, with reference to those of the cells with the film of TNWs or TNPs. The slightly higher V_{OC} of the DSSC with the composite film is owing to the inner TNWs, which can provide better pathways for electron transfer than TNPs. The cell with the composite film of TNWs/TNPs shows a light-harvesting efficiency of 3.04%; on the other hand, the cell with pure TNWs and pure TNPs show of only 1.59% and 1.67% of efficiency respectively.

3.3 EIS analysis

EIS (Electron impedance spectroscopy) is used to measure the charge transfer resistance of the electrode materials for characterizing the separation efficiency of the photogenerated electron-hole pairs [29], [30]. The typical nyquist plot of the impedance data for all DSSCs were studied and shown in Fig.3.5. Generally, all the nyquist spectra of DSSCs exhibit three semicircles, which are assigned to electron transport at the counter electrode (Z_1-higher frequency region), charge transfer process at the TiO_2/dye/electrolyte interface (Z_2-mid frequency region) and Warburg diffusion process of I^-/I_3^- within the electrolyte (Z_3-lower frequency region) respectively. By modeling and fitting the nyquist plots with equivalent circuit model, the electron transport parameters, such as serial ohmic resistance (R_s), electron transport resistance R_{ct} at counter electrode/electrolyte interface, charge transfer resistance R_{rec} at the TiO_2/dye/electrolyte interface, electron diffusion impedance Z_d, effective electron life time (τ_{eff}), electron diffusion length (L_n) and effective diffusion coefficient (D_{eff}) were extracted. In addition, C_{ct} is interfacial capacitance at the interface of counter electrode/electrolyte and C_{rec} is a chemical capacitance representing the change of electron density as a function of the Fermi level are measured. An equivalent circuit used to fit the experimental data is shown in Fig. 3.6. This equivalent circuit is based on the diffusion–recombination model proposed and has been frequently employed to analyze similar structures [31], [32], [33]. The resistance elements R_{ct}, R_{rec} and Z_d were described as real parts of Z_1, Z_2, and Z_3 respectively. In general the first and third semicircles are weak when compared the second semicircle. This largest semi-circle represents interfacial charge transfer resistance, R_{rec}, of the injected electrons to the direct transfer from the TiO_2 NWs to I_3^- ions at the TiO_2/dye/electrolyte interface. The extracted R_s, R_{rec}, R_{ct}, C_{rec}, C_{ct}, Z_d, τ_{eff} , D_{eff} and L_n values are presented in Table 3.2. Estimations of D_{eff} and L_n were done using equations [34]:

$$D_{eff} = (R_{ct}/R_{rec})(L_F^2/\tau_{eff})$$

$$Ln = (\tau D_{eff})^{1/2}$$

where L_F represents the film thickness of the anode.

From the Fig. 3.5, comparison of the middle semicircles of the DSSCs indicates the decrease of the diameter in the order DSSC-1>DSSC-6>DSSC-2>DSSC-5>DSSC-4>DSSC-3, suggesting that DSSC-3 contribute to the lowest charge recombination at the TiO_2/dye/electrolyte interface. The lowest value of the R_{rec} for 10% TNWs suggested higher surface area of the TNW/TNP photoanode and more adequate pore sizes for facile transport of the redox couple in the TNP interface thereby reducing the corresponding resistance at the interface since the TNW had a higher surface area than the TiO_2 NPs [35]. The DSSC based on pure TNWs, however, showed a poorer performance than that of the DSSC based on pure TNPs. In this study, higher efficiencies were achieved for DSSCs based on TNWs/TNPs hybrids from 10 to 90 wt% than the cell based on pure TiO_2 NPs and pure NWs. The DSSCs made of composite TNW/TNP has higher chemical capacitance at the TiO_2/dye/electrolyte interface, larger effective electron life time, longer electron diffusion length and elevated effective diffusion coefficient when compared to other DSSCs. These results were indicated that reduction of the electron recombination and increase electron transport at the /dye/electrolyte interface. The enhanced efficiency of these TNWs/TNPs hybrid DSSCs is achieved by optimizing device architectures, that enhance light absorption and facilitate electron transport by determining and designing appropriate dimensions of TiO_2 NWs, by optimizing the cation concentration in the electrolyte solution for promoting electron injection yield from sensitizing indigo carmine dye molecules to hybrid TiO_2 electrodes, or by

synthesizing thermally stable TNWs with a stable high surface area. In the composite TNWs/TNPs photo electrode, the lower R_{rec} suggesting that each nano tubule makes more difficult for an electron to jump outside the nanostructure than to stay within the structure during diffusion; this explains the high collection efficiencies and thus high short-circuits photocurrents.

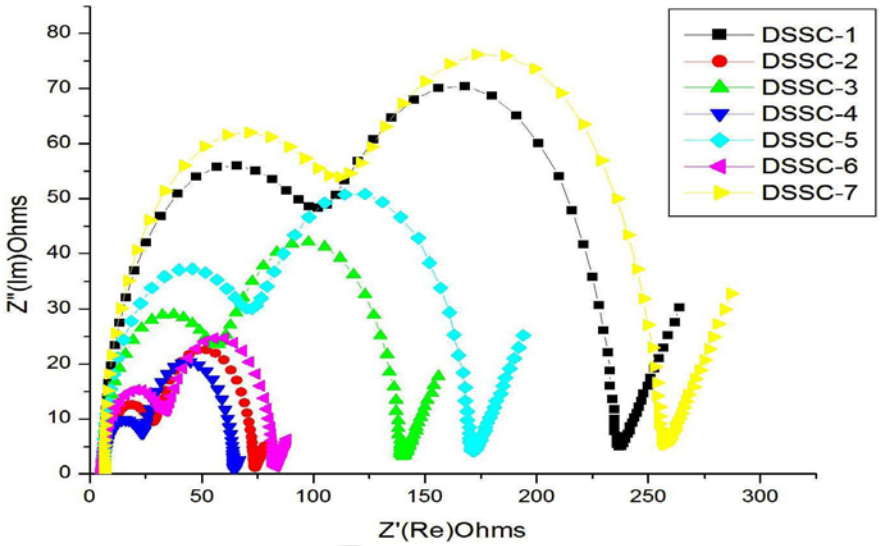

Fig 3.5 Typical nyquist plot of Electrochemical Impedance Spectroscopy (EIS) of DSSCs

The size of the semicircle at low frequency becomes much smaller after mixing 10% nanowires in the photoanode when compared to the pure TNPs photoanode as shown in Fig. 3.5, indicating a lower resistance of the electron transfer at the electrolyte interface. The lower resistance in this interface suggested that nanowires in the photoanode could reduce the charge recombination and promote the electron transfer because of their one-dimensional structure. However, the pure nanowire electrode displays a much larger semicircle at low frequency, even larger than that of the pure TNPs electrode. This should be owing to its poor dye absorption and blocking of electron transport in the photoanode. From the Table 3.2, it could be observed that, R_{ct} values decreases steeply up to 10% of TNW content. This decrease indicates clearly that electron transport in the titania electrode is improved by mixing TNWs with TNPs. The ratio of R_{rec} and R_{ct} decreases with increase of TNWs content with the TNPs. This shows that TNWs restrains the recombination reactions between electrons in the titania electrode and I_3^- ions in the electrolyte and contributes to collect electrons properly to the transparent conducting glass electrode.

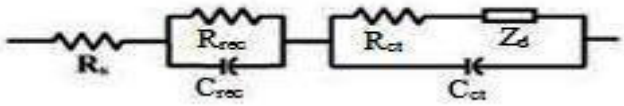

Fig 3.6 An equivalent circuit diagram of Electrochemical Impedance Data (EIS)

The experimental results of I-V and EIS measurements of DSSCs made of composite TNWs/TNPs photoanode clearly showed the following three points, 1) Resistance of electron transport in the titania electrode R_{ct} is small for DSSC-3. 2) The ratio of resistance R_{rec}/R_{ct} is large indicate high electron collection efficiency. 3) Electron density in the titania electrode is high. From these results it can be concluded that the optimized composite of TNWs with TNPs exhibit different semiconductor electrochemical behaviours when they are employed in dye-sensitized solar cells. In this photoelectrochemical system, charge separation, transport, and recombination strongly depend on the nanostructures in the photoanode. From EIS data it can be observed that for the cell containing TiO_2 nanowires, formation of a space charge layer at the surface of the electrode effectively promotes the separation of photogenerated charge carriers and prevents recombination of

the electron with the hole carriers. The uninterrupted long pathway with fewer boundaries is beneficial for transport of electron towards the conducting substrate.

Table 3.1: Photovoltaic parameters of DSSCs made of various concentrations of TNWs with TNPs.

DSSCs	V_{OC} (mV)	I_{SC} (mA)	V_{MAX} (mV)	I_{MAX} (mA)	FF (%)	η (%)
DSSC-1	800	7.2	700	5.2	63.19	0.91
DSSC-2	840	11	740	9	72.08	1.67
DSSC-3	880	17.1	810	15	80.74	3.04
DSSC-4	870	15.4	790	13	76.65	2.57
DSSC-5	860	13.2	770	11	74.61	2.12
DSSC-6	850	10.3	790	8.1	73.09	1.59

Simultaneously, the decrease of trap sites in the band gap and the surface state can effective enhance the charge-diffusion coefficient and suppression of the interfacial charge transfer. In the present investigation, with an optimized ratio of TNWs/TNPs in the photo electrode, an enhancement of energy conversion of ~ 82% is achieved in the DSSC–3, as compared with that consisting of pure TiO_2 NPs (DSSC-2). DSSC-3 is found to have the lowest resistance among the other cells, namely the minimum R_{rec} and R_{ct} resistance. These results reflected more efficient electron transfer at TiO_2/dye/electrolyte interface and the redox electrolyte/counter electrode interfaces. In addition, the nanostructure prevents recombination of electron at TiO_2/dye/electrolyte. It should be pointed out that pure TNWs film based cell has highest R_{rec} and R_{ct} resistance among the other nano structured cells. Possible reason is that TNWs-based cell has relatively disordered film structure stemmed from the random agglomeration of TiO_2 NWs, and hence resulting in a loose mechanical contact between TNWs layer and conducting glass plate. The poor contact between film layer and glass substrate might lead to the high resistance and low conversion efficiency.

Table 3.2: Electron transport parameters of electrochemical impedance spectroscopy obtained from the nyquist plot.

DSSCs	R_s Ω	R_{rec} Ω	R_{ct} Ω	C_{rec} μF	C_{ct} μF	Z_d $\Omega.s^{-0.5}$	τ_{eff} μs	D_{eff} cm^2/s 10^{-4}	L_n μm
DSSC-1	4.999	20.00	12.00	26.02	0.50	0.50	520	46.12	15.49
DSSC-2	4.997	16.01	6.90	39.2	1.20	0.40	627	53.24	18.28
DSSC-3	5.001	7.99	1.50	101.00	2.50	0.10	808	94.96	27.71
DSSC-4	4.998	11.00	3.00	70.03	1.80	0.20	770	68.52	22.97
DSSC-5	4.999	13.01	4.99	50.03	1.49	0.30	650	57.63	19.37
DSSC-6	5.000	17.01	7.40	36.70	0.99	0.43	624	53.02	18.19

4. CONCLUSION

The experimental results show that the composite photoanode is an innovative electrode that can noticeably improve the performances of the solar cell. Under the same fabrication conditions and film thickness, the solar cell made with the composite electrode containing 10 wt %, 50 wt% and 90 wt % nanowires with TiO_2 nanoparticles demonstrated 82%, 54% and 27% of higher device efficiency than that made using pure TiO_2 nanoparticles. Thus by rational tuning the weight ratio of TNWs and TNPs, the DSSC-3 had the highest η value, which was increased about 82% compared to DSSC-2 (pure TiO_2 NP solar cell). It was believed that the power conversion efficiency of composite solar cells was attributed to the dye adsorption amount and the interfacial charge transfer. In addition, the nanowires in the electrode cannot only provide a straight path for electron transport but also function as scattering particles to increase light harvesting efficiency, which leads to an improvement of efficiency as compared to the cell made with the pure TiO_2 electrode. The results of the current investigation indicate the present TiO_2 nanowire is promising in enhancing the performance of dye sensitized solar cells. The cell performance confirms that the TiO_2 NWs/NPs composite can suppress the charge recombination process effectively and improve the overall conversion efficiency. From this investigation it could concluded that the application of TNWs/TNPs composite photoanode can promote the interfacial electron transfer and suppress the electron recombination effectively. In addition the sensitizer indigo carmine dye, electrolyte PMII and counter electrode material copper sulfide given better results for DSSCs fabrication.

ACKNOWLEDGMENT

The authors are thankful to the authorities of Annamalai University, for providing all necessary facilities to carry out the present work successfully.

REFERENCES

[1] J.A. Anta,"Electron transport in nanostructured metal-oxide semiconductors," *Current Opinion in Colloid and Interface Science,* vol. 17, no. 3, pp. 124-131, Jun. 2012.

[2] Hagefldt, G. Boschloo, L. Sun, L. Kloo, and H. Pettersson, "Dye-sensitized solar cells," *Chem. Rev,* vol. 110, no. 11, pp. 6595-6663, Sep. 2010.

[3] M. Grätzel, "Photoelectrochemical cells," *Nature,* vol. 414, no. 6861, pp. 338–344, Nov. 2001.

[4] O.K. Varghese, M Paulose, and C.A Grimes, "Long vertically aligned titania nanotubes on transparent conducting oxide for highly efficient solar cells," *Nat Nanotechnol,* vol. 4, no.9, pp. 592-597, Sep. 2009,

[5] F. Xu, M. Dai, Y. Lu, and L. Sun, "Hierarchical ZnO Nanowire-Nanosheet Architectures for High Power Conversion Efficiency in Dye-Sensitized Solar Cells," *J. Phys. Chem. C,* vol. 114, no. 6, pp. 2776–2782, Jan. 2010.

[6] C. Xu, J. Wu, U.V. Desai, and D. Gao, "Multilayer Assembly of Nanowire Arrays for Dye-sensitized Solar Cells," *J. Am. Chem. Soc,* vol. 133, no. 21, pp. 8122-8125, Apr. 2011.

[7] D. Hwang, S.M. Jo, D.Y. Kim, V. Armel, D.R. MacFarlane, and S.Y. Jang, "High Efficiency Solid-state Dye-sensitized Solar Cells Using Hierarchically Structured TiO_2 Nanofibers," *ACS Appl. Mater. Interface,* vol. 3, no. 5, pp. 1521-1527, 2011.

[8] B. Oregan, and M. Gratzel," A low-cost, high-efficiency solar cell based on dye-sensitized colloidal TiO2 films," *Nature,* vol. 353, pp. 737-740, Oct. 1991.

[9] M. Gratzel, "Recent Advances in Sensitized Mesoscopic Solar Cells,"*Acc. Chem.Res,* vol. 42, no. 11, pp.1788–1798, Nov. 2009.

[10] J.T. Park, D.K. Roh, R. Patel, K.J. Son, W.G. Koh, and J.H. Kim, "Fabrication of hole-patterned TiO_2 photoelectrodes for solid-state dye-sensitized solar cells," *Electrochimica Acta,* vol. 56, no. 1, pp. 68–73,

Dec. 2010.

[11] F. Shao, J. Sun, L. Gao, S. Yang, and J. Luo, "Growth of Various TiO_2 Nanostructures for Dye-Sensitized Solar Cells," *J. Phys. Chem. C,* vol. 115, no. 5, pp. 1819–1823, 2011.

[12] Y. Wang, H. Yang, and H. Xu, "DNA-like dye-sensitized solar cells based on TiO_2 nanowire-covered nanotube bilayer film electrodes," *Materials Letters,* vol. 64, no. 2, pp. 164–166, Oct. 2010.

[13] B. Liu, and E.S. Aydil, "Growth of Oriented Single-Crystalline Rutile TiO_2 Nanorods on Transparent Conducting Substrates for Dye-Sensitized Solar Cells," *J. Am. Chem. Soc,* vol. 131, no. 11, pp. 3985–3990, 2009.

[14] H. Wang, Y. Bai, H. Zhang, Z. Zhang, J. Li, and L. Guo, " Cds quantum dots-sensitized TiO_2 nanorod array on transparent conductive glass photoelctrodes," *J, Phys. Chem. C,* vol. 114, no. 7, pp. 16451-16455, Sep. 2010.

[15] M. Law, L.E. Greene, J.C. Johnson, R. Saykally, and P. Yang, "Nanowire dye- sensitized solar cells," *Nature Materials*, vol. 4, pp. 455 - 459, 2005.

[16] K.H. Yu, and J. H. Chen, "Enhancing Solar Cell Efficiencies through 1-D Nanostructures," *Nanoscale Research Letters*, vol. 4, no. 1, pp. 1-10, 2009.

[17] M.K. Nazeeruddin, F. De Angelis, S. Fantacci, A. Selloni, G. Viscardi, P. Liska, S. Ito, B. Takeru, and M.Grätzel, "Combined experimental and DFT-TDDFT computational study of photoelectrochemical cell ruthenium sensitizers," *J. Am.Chem. Soc,* vol. 127, no. 48, pp. 16835–16847, Dec. 2005.

[18] A.C. Fisher, L.M. Peter, E.A. Ponomarev, A.B. Walker, and K.G.U. Wijayantha, "Intensity Dependence of the Back Reaction and Transport of Electrons in Dye-Sensitized Nanocrystalline TiO_2 Solar Cell," *J. Phys. Chem. B*, vol. 104, no. 5,pp. 949-958, Feb. 2000.

[19] J. Nissfolk, K. Fredin, A. Hagfeldt, and G. Boschloo, "Recombination and Transport Processes in Dye-Sensitized Solar Cells Investigated under Working Conditions," *J, Phys. Chem. B,* vol. 110, no. 36, pp. 17715-17718, Sep. 2006.

[20] Y. Zhang, Z. Xie, and J. Wang, "Supramolecular-templated thick mesoporous titania films for dye-sensitized solar cells: effect of morphology on performance," *ACS Appl. Mater Interfaces,* vol. 1, no. 12, pp. 2789-95, Dec. 2009.

[21] A.J. Frank, N. Kopidakis, and V.D. Lagemaat," Electrons in nanostructured TiO_2 solar cells: transport, recombination and photovoltaic properties," *J.Coord. Chem. Rev.,* vol. 248, pp. 1165-1179, Mar. 2004.

[22] A. Kokil, A. Renna, J. Kumar, and S. Granados-Focil, "Synthesis and Characterization of Triazolium Iodide IonicLiquid Electrolyte for Dye Sensitized Solar Cells," J. Macromolecular Sci, Part A: Pure and Applied Chemistry, vol. 48, no. , pp. 1022–1026, Nov. 2011.

[23] G. Armstrong, A.R. Armstrong, J. Canalesa, and P.G. Bruce,"Nanotubes with the TiO_2-B structure," *Chem. Commun.,* vol. 21, no. 19, pp. 2454-2456, May. 2005.

[24] C.H. Lee, S.W. Rhee, and H.W. Choi, "Preparation of TiO_2 nanotube/nanoparticle composite particles and their applications in dye-sensitized solar cells," *Nanoscale Res Lett.* vol. 7, pp. 48-52, Jan. 2012.

[25] http://www.earthues.com/

[26] M. Gillet, R. Delamare, and E. Gillet, "Growth of epitaxial tungsten oxide nanorods," *J. Crystal Growth*, vol. 279, no. 1–2, pp. 93-99, May. 2005.

[27] H. Hafez, M. Saif, and M.S.A. Abdel-Mottaleb, "Down-converting lanthanide doped TiO_2 photoelectrodes for efficiency enhancement of dye-sensitized solar cells," *J. Power Sources*, vol. 196, no. 13, pp.5792-5796, July. 2011.

[28] J. Yu, J. Fana, and Z. Li, "Dye-sensitized solar cells based on hollow anatase TiO_2 spheres prepared by self-transformation method," *Electrochimica Acta*, vol. 55, no. 3, pp. 597-602, Jan. 2010.

[29] K. Shankar, I. Basham, N.K. Allam, O.K. Varghese, G.K. Mor, X. Feng, M. Paulos, A. Seabold, S.C. Ky, and C.A. Grimes," Recent advances in the use of TiO_2 nanotube and nanowire arrays for oxidative photoelectrochemistry," *J. Phys. Chem B*, vol. 113, no. 16, pp. 6327-6359, Mar. 2009.

[30] J. Wang, Y. Han, M. Feng, J. Chen, X. Li, and S. Zhang, " Preparation and photoelectrochemical characterization of WO_3/TiO_2 nanotube array electrode," J. Mater. Sci, vol. 46, no. 2, pp. 416-421, Jan. 2011.

[31] W.H. Leng, Z. Zhang, J.Q. Zhang, and C.N. Cao, "Investigation of the kinetics of a TiO_2 photoelectrocatalytic reaction involving charge transfer and recombination through surface states by electrochemical impedance spectroscopy," *J. Phys. Chem B*, vol. 109, no. 31, pp. 15008-15023, Aug. 2005.

[32] Y. Zhang, X. Li, M. Feng, F. Zhou, and J. Chen, "Photoelectrochemical performance of TiO_2-nanotube-array film modified by decoration of TiO_2 via liquid phase deposition," *Surface & Coatings Technology*, vol. 205, no. 7, pp. 2572-2577, Dec. 2010.

[33] B. Tan, and Y. Wu, "Dye-Sensitized Solar Cells Based on Anatase TiO_2 Nanoparticle/Nanowire Composites," *J. Phys. Chem. B*, vol. 110, pp.15932-15938, July. 2006.

[34] J. Bisquert," Theory of the Impedance of Electron Diffusion and Recombination in a Thin Layer, " *J. Phys. Chem. B*, vol. 106, no. 2, pp. 325–333, Dec. 2001.

[35] M. Adachi, M. Sakamoto, J. Jiu, Y. Ogata, S. Isoda, "Determination of Parameters of Electron Transport in Dye-Sensitized Solar Cells Using Electrochemical Impedance Spectroscopy," *J, Phys. Chem. B*, vol. 110, no. 28, pp. 13872-13880, July. 2006.